DOI: 10.26599/FSHW.2026.9251258

Contents lists available at SciOpen

Food Science and Human Wellness

journal homepage: https://www.sciopen.com/journal/2097-0765

China Food Publishing Co.

Bifidobacterium adolescentis CCFM1061 Modulates Gut Microbiota and Alleviates Hepatic Lipid Accumulation: A Randomized, Double-Blind, Placebo-Controlled Trial

Yuheng Wu[a,c#], Jiyuan Ge[b#], Yeping He[d], Xuhua Mao[a,c,e], Dongbo Yuan[e], Lei Sun[a,c], Qingyue Lan[b], Feng Hang[a,c,g], Qixiao Zhai[a,c,f], Wei Chen[a,c,f], Gang Wang[a,c,f,g,h*], Yifeng Luo[b*]

[a] *State Key Laboratory of Food Science and Resources, Jiangnan University, Wuxi 214122,China*

[b] *Department of Radiology, the Affiliated Yixing Hospital of Jiangsu University, Wuxi 214200, China*

[c] *School of Food Science and Technology, Jiangnan University, Wuxi 214122, China*

[d] *Department of Ultrasound, the Affiliated Yixing Hospital of Jiangsu University, Wuxi 214200, China*

[e] *Department of Clinical Laboratory, the Affiliated Yixing Hospital of Jiangsu University, Wuxi 214200, China*

[f] *National Engineering Research Center for Functional Food, Jiangnan University, Wuxi 214122, China*

[g] *(Yangzhou) Institute of Food Biotechnology, Jiangnan University, Yangzhou 225004,China*

[h] *Wuxi Institute for Specialized nutrition and Health Co., Ltd., Wuxi 214142, China*

ABSTRACT: Metabolic dysfunction–associated fatty liver disease (MAFLD) has become the most prevalent chronic liver disease worldwide. Its management remains challenging due to poor adherence to long-term lifestyle interventions and the absence of clinically approved, specific pharmacological treatments. Probiotic approaches targeting the gut-liver axis have therefore emerged as promising therapeutic strategies. This randomized, double-blind, placebo-controlled trial enrolled 100 adults with MAFLD who received either 1×10^{10} CFU of *Bifidobacterium adolescentis* CCFM1061 (n = 50) or a placebo (n = 50) daily for 13 weeks. Hepatic fat content was quantified using magnetic resonance imaging-proton density fat fraction (MRI-PDFF), combined with 16S rRNA gene sequencing and non-targeted metabolomic profiling of fecal and serum samples to enable integrated multi-omics evaluation. Compared with placebo, CCFM1061 supplementation significantly reduced hepatic fat accumulation in the left lateral superior, anterior inferior, posterior inferior, and posterior superior liver segments. No significant changes were observed in liver function indicators, lipid parameters, or blood glucose levels. CCFM1061 intervention enriched beneficial gut taxa, including Bacteroides. Metabolomic analysis revealed increased fecal primary bile acids (taurocholic acid and taurochenodeoxycholic acid) and decreased serum markers of fatty acid oxidation (e.g., suberic acid) and branched-chain amino acid metabolism (e.g., N-isovalerylglycine). Multi-omics correlation analysis demonstrated coordinated associations between gut microbiota remodeling, bile acid profiles, systemic metabolic features, and region-specific hepatic fat reduction, as assessed by MRI-PDFF. Together, these findings indicate that CCFM1061 supplementation is associated with improved hepatic lipid accumulation and support a gut–liver axis–centered interpretative framework for probiotic intervention in MAFLD.

[#] Yuheng Wu and Jiyuan Ge contributed equally to this work and should be considered co-first authors.
***Corresponding author**
wanggang@jiangnan.edu.cn (G.Wang);
staff1277@yxph.com (Y.F. Luo)

Received 9 December 2025
Received in revised from 30 January 2026
Accepted 9 April 2026

Keywords: *Bifidobacterium adolescentis*; Metabolic dysfunction-associated fatty liver disease; MRI-PDFF; Gut-liver axis; Gut microbiota

1. Introduction

Metabolic dysfunction–associated fatty liver disease (MAFLD) is a metabolic disorder characterized by hepatic steatosis in the presence of overweight/obesity, type 2 diabetes mellitus, or other metabolic abnormalities, representing the hepatic manifestation of systemic metabolic dysfunction. The disease spectrum of MAFLD ranges from simple steatosis to metabolic-associated steatohepatitis, progressive fibrosis, and even cirrhosis[1,2]. Epidemiological evidence demonstrates that metabolic dysfunction–associated fatty liver disease (MAFLD) has emerged as the leading chronic liver condition worldwide, affecting approximately 25% of adults[3]. Its increasing prevalence among younger populations and the associated substantial health burden have established MAFLD as a critical public health challenge[4]. Currently, no pharmacotherapies are specifically approved for MAFLD management. Although lifestyle interventions serve as first-line treatment and demonstrate efficacy, patient compliance remains poor and therapeutic outcomes are limited[5].

The liver does not function in isolated; its physiological status is intimately linked with the gastrointestinal tract. The "gut-liver axis" concept has provided novel insights into the pathogenic mechanisms underlying MAFLD. Studies indicate that patients with MAFLD commonly present with the gut microbiota imbalance characterized by diminished microbial diversity[6]. This dysbiosis typically involves overabundance of opportunistic pathogens (e.g., *Escherichia coli*, *Prevotella*, and *Streptococcus*) alongside decline in beneficial genera such as *Faecalibacterium*, *Coprococcus*, and *Ruminococcus*[7]. This dysbiosis contributes to hepatic steatosis, inflammation, and fibrosis through multiple mechanisms: disrupting the intestinal barrier and increasing intestinal permeability[8,9], elevating endotoxin entry into the bloodstream[10], and impairing synthesis of beneficial metabolites including bile acids[11] and short-chain fatty acids[12]. Consequently, modulating the gut microbiota represents a promising therapeutic avenue for MAFLD intervention.

Probiotics demonstrate unique advantages due to their favorable safety profile and capacity to regulate gut microbiota. Animal studies have confirmed that *Bifidobacterium*-derived metabolites, such as lactic acid, can ameliorate diet-induced lipid metabolism disorders in MAFLD by suppressing NLRP3 inflammasome-related inflammatory responses and regulating autophagy pathways[13]. Additional evidence suggests that *Bifidobacteria* mitigate insulin resistance and hepatic lipid deposition in MAFLD mouse models through simultaneous engagement of hepatic Farnesoid X receptor (FXR) signaling and inhibition of its intestinal counterpart[14]. Furthermore, bile salt hydrolase (BSH) produced by Bifidobacteria deconjugates primary bile acids—a process considered crucial for subsequent bile acid transformation—and improves hepatic fat accumulation by regulating the gut-liver axis[15]. *Bifidobacterium adolescentis* FJSSZ23M10 reduced body weight in high-protein-induced obese mice, improved serum lipid profiles, alleviated adipose tissue lipid accumulation, and regulated energy metabolism, while significantly increasing gut *Bifidobacterium* species and butyrate levels[16]. However, most findings remain at the preclinical stage, with insufficient exploration of their efficacy and underlying mechanisms in human clinical settings.

Preliminary studies indicate that *Bifidobacterium adolescentis* CCFM1061 demonstrates multiple therapeutic effects in animal models of type 2 diabetes: it significantly improves glucose metabolism, effectively reduces fasting blood glucose, and ameliorates insulin resistance. Simultaneously, this strain elevates murine concentrations of short-chain fatty acids (including acetic, propionic, butyric, and isobutyric acids) while concurrently lowering levels of low-density lipoprotein, hepatic triglycerides, and total liver cholesterol. Histological analysis further confirmed that *B. adolescentis* CCFM1061 mitigates disease-induced pathological damage in the liver and pancreas while significantly reducing inflammatory levels in hepatic tissue, establishing a crucial theoretical foundation for investigating *B. adolescentis* CCFM1061's intervention potential in MAFLD patients[17,18]. To assess its effectiveness in humans and elucidate underlying mechanisms, we designed and implemented a randomized, double-blind, placebo-controlled clinical trial. Liver biopsy, considered the gold standard, is challenging to apply in large-scale screening and dynamic monitoring due to its invasiveness and sampling errors. Among non-invasive examinations, ultrasound exhibits insufficient sensitivity for detecting mild fatty liver disease and yields operator-dependent results; computed tomography involves ionizing radiation and cannot accurately distinguish between fat and iron deposits; conventional magnetic resonance imaging with in-phase/out-of-phase techniques is susceptible to interference from hepatic iron overload[19]; while magnetic resonance spectroscopy is accurate, it typically employs single-element sampling, resulting in limited coverage and difficulty reflecting global heterogeneity of hepatic fat deposition[20]. Therefore, this study employed MRI-PDFF for quantitative assessment of hepatic fat. This technique enables non-invasive, radiation-free, and precise fat quantification across multiple regions of the entire liver, effectively overcoming limitations of aforementioned methods and providing a reliable technical foundation for objectively and sensitively evaluating probiotic intervention effects[21]. Furthermore, the study design integrates 16S rRNA-based gut microbiota sequencing with untargeted metabolomic analyses of fecal and serum samples to enable comprehensive evaluation of the clinical effects of *B. adolescentis* CCFM1061, aiming to establish a viable and efficacious strategy for probiotic-assisted reduction of hepatic lipid accumulation in MAFLD patients.

Notably, although multiple microbial and metabolic pathways have been implicated in the pathogenesis of MAFLD, the mechanistic basis underlying probiotic intervention in human studies remains incompletely defined. Existing clinical and translational studies often report alterations in gut microbiota composition, bile acid profiles, or host metabolic signaling, yet these observations are frequently interpreted in isolation rather than within a unified mechanistic framework linking the gut and liver[22].Accumulating evidence suggests that remodeling of gut microbiota may represent an upstream event in metabolic regulation, giving rise to changes in gut-derived metabolites that subsequently influence hepatic lipid handling and metabolic homeostasis[23]. Among these metabolites, bile acids have emerged as key signaling molecules mediating gut–liver communication, capable of modulating hepatic lipid metabolism, mitochondrial function, and metabolic flexibility through receptor-dependent and receptor-independent pathways[24–26].

In this context, the present study adopts a gut–liver axis–centered framework, proposing that *B. adolescentis* CCFM1061 primarily exerts its beneficial effects through modulation of gut microbiota structure and associated metabolic outputs, particularly bile acid profiles, which are linked to improvements in hepatic fat accumulation. This conceptual framework guided the integrated application of MRI-PDFF imaging and multi-omics analyses in the current randomized, double-blind, placebo-controlled trial.

2. Materials and methods

2.1. Participant Enrollment and Ethical Compliance

This randomized, double-blind, placebo-controlled trial was conducted in accordance with the ethical principles outlined in the Declaration of Helsinki and applicable clinical research regulations. Prior to commencement, the study protocol received review and approval from the Medical Ethics Committee of Yixing People's Hospital, Jiangsu Province, China (Approval No.: 2024 Ethics Review No. 080-01) and was registered with the China Clinical Trial Registry (ChiCTR2400093124). All participants provided written informed consent before undergoing any study-related procedures. Recruitment, intervention, and follow-up activities were conducted at Yixing People's Hospital.

2.2. Inclusion and exclusion criteria

Inclusion criteria were as follows: (A) diagnosis of metabolic dysfunction-associated fatty liver disease (MAFLD) based on established diagnostic criteria; (B) age 18–65 years, regardless of sex; (C) demonstrated adequate adherence to follow the clinical trial protocol; (D) provision of written informed consent by the participant or legal guardian; (E) willingness and ability to complete all baseline assessments (informed consent, International Physical Activity Questionnaire, dietary survey) and cooperate with all study procedures throughout the trial duration.

Exclusion criteria were as follows: (A) alcohol consumption exceeding 40 g per week (ethanol equivalent); (B) regular use within the preceding 6 months of medications including nonsteroidal anti-inflammatory drugs, antibiotics, corticosteroids, antineoplastic or antituberculosis agents, or specific herbal/mineral preparations (e.g., nux vomica/arsenic trisulfide); (C) history of substance abuse involving narcotics, psychotropic drugs, or tobacco within the past 6 months; (D) recent (past 6 months) use of drugs known to influence study outcomes or hepatic metabolism, such as gastric acid suppressants, amiodarone, valproate, prednisone, tamoxifen, piroxicam, methotrexate, known hepatotoxic agents, hormonal therapies, statins, antihypertensive medications, or ursodeoxycholic acid; (E) frequent supplementation (≥2 times weekly) during the study or in the 3 months prior with probiotics, multivitamins/minerals, or antioxidants; (F) presence of comorbid conditions that could confound hepatic assessment or participant safety, including but not limited to other primary liver pathologies (cholestasis, transplant history), systemic acute illness, cystic fibrosis, muscular/neurological dystrophies, significant gastrointestinal abnormalities, heart failure, thyroid disorders, inflammatory bowel disease, renal or respiratory failure, hereditary conditions affecting the liver (hemochromatosis, Wilson's disease, α-1 antitrypsin deficiency), autoimmune diseases, celiac disease, or any

malignancy; (G) significant weight loss (>5% body weight) within the last 6 months, history of total parenteral nutrition, or protein-calorie malnutrition; (H) pregnancy or lactation; (I) known allergy or hypersensitivity to any ingredient in the investigational probiotic product; (J) contraindications to undergoing magnetic resonance imaging-proton density fat fraction (MRI-PDFF), such as incompatible metallic implants (e.g., pacemakers, neurostimulators, cochlear implants, aneurysm clips), severe claustrophobia, or conditions (e.g., uncontrolled tremor, cognitive impairment) that would preclude cooperation during the MRI scan.

2.3. Discontinuation, withdrawal, and termination criteria

Post-enrollment exclusion criteria were as follows: (A) participants who were identified during the trial as not meeting the predefined inclusion criteria despite enrollment, including but not limited to enrollment errors, inaccurate diagnosis, failure to receive the assigned investigational product, or absence of complete assessment and follow-up data; (B) participants with protocol violations that precluded valid efficacy evaluation. For all excluded cases, the specific reasons for exclusion were documented, and relevant original records were retained for verification. Excluded participants were not included in the efficacy analysis; however, participants who received at least one intervention and had available safety-related data were included in the safety analysis.

Withdrawal and loss-to-follow-up criteria were as follows: (A) voluntary withdrawal of informed consent by the participant; (B) loss to follow-up during the intervention or assessment period; (C) insufficient compliance with the study protocol; or (D) discontinuation recommended by the investigators due to comorbidities or other medical considerations. The specific reason for withdrawal or loss to follow-up was recorded for each participant. For participants who obtained partial efficacy-related data prior to withdrawal, the last available valid assessment was used for statistical analysis.

Criteria for premature termination of the trial were as follows: (A) identification of potential safety risks during the study; (B) insufficient intervention efficacy or occurrence of serious adverse events; (C) inadequate research funding or administrative support; or (D) requirements from regulatory or administrative authorities. In the event of premature trial termination, all data, documents, and records generated during the study were systematically organized and securely archived to ensure traceability of the research process.

2.4. Sample size calculation, study design, randomization and masking

The required sample size was calculated using G*Power, version 3.1 (Figure S1). Effect sizes were derived from previous studies[27]. To achieve a statistical power of 0.8, each group required 34 volunteers to detect an effect size $d = 0.612$ at $\alpha = 0.05$. Accounting for a 25% dropout rate, a minimum of 45 volunteers per group was necessary.

This trial was conducted from November 2024 to June 2025 at Yixing People's Hospital in Jiangsu Province, China. The trial comprised two randomly assigned parallel groups: the *Bifidobacterium adolescentis* CCFM1061 group and the placebo group. Participants were instructed to take one packet of the product with warm water (≤37 °C) 30 minutes after breakfast and dinner daily. Participants' lifestyles were regularly

monitored to ensure no significant changes in dietary habits occurred during the 13-week trial period. The duration of the study and the probiotic dosage were determined based on prior research findings[28].

Randomization was conducted using sealed envelopes. After recording relevant data, the principal investigator opened the envelopes. The double-blind principle was maintained by ensuring no differences in appearance or packaging between the two products. The trial list was revealed only after completing the trial and determining all experimental indicators.

2.5. Study products

Both the probiotic and placebo products were manufactured by the (Yangzhou) Institute of Food Biotechnology (Jiangsu Province, China) using identical stick-pack packaging (2 g per pack). The probiotic product contained *B. adolescentis* CCFM1061 at a concentration of 2.5×10^9 CFU/g, with maltodextrin as the excipient. The placebo product consisted of maltodextrin without *B. adolescentis* CCFM1061 (since the bacterial biomass constituted a negligible proportion of the total product mass, the weight of the placebo remained approximately 2 g despite the absence of bacteria). The two products were indistinguishable in weight, appearance, color, taste, and odor, ensuring effective blinding of both participants and investigators throughout the study. Product allocation was concealed using coded labeling, with the code remaining undisclosed until completion of data analysis. Participants assigned to the probiotic group orally ingested one sachet of the probiotic product twice daily, while those in the placebo group received one sachet of the placebo product twice daily.

All products complied with the GB/T 29602 implementation standard and were stored at temperatures below 4 °C during the intervention period. The shelf life of both products was one year.

2.6. Sample collection and clinical laboratory testing

All MAFLD participants underwent comprehensive health examinations at Yixing People's Hospital prior to intervention. Fasting blood and stool specimens were collected at two time points: baseline (day 1) and study completion. Serum was separated via centrifugation (3500 r/min, 10 minutes) for clinical laboratory testing. Fecal samples were collected into sterile containers and immediately stored at −80°C for subsequent analyses. Blood biochemistry profiling was performed using a Hitachi LABOSPECT 008A fully automated biochemical analyzer (Japan). All assay reagent kits were obtained from Ningbo Ruiyuan Biotechnology Co., Ltd. (China). Serum biochemical parameters were measured using standardized automated assays. Aspartate aminotransferase (AST) and alanine aminotransferase (ALT) activities were determined using substrate-based methods, while γ-glutamyl transferase (GGT) was analyzed using a GPNA substrate. For lipid profiling, total cholesterol (TC) and triglyceride (TG) concentrations were measured using the CHOD-PAP and GPO-PAP methods, respectively. High-density lipoprotein cholesterol (HDL-C) and low-density lipoprotein cholesterol (LDL-C) levels were determined via the direct hydrogen peroxide elimination method and the selective elimination method, respectively. Free fatty acids (FFA) were quantified using an enzymatic colorimetric assay. For metabolic and inflammatory markers, glucose (GLU) was measured using the glucose oxidase method, high-sensitivity C-reactive protein (hs-CRP) and glycated hemoglobin (HbA1c) were quantified by

latex immunoturbidimetry, and insulin was assessed using a chemiluminescence immunoassay. The atherosclerosis index (AI) was calculated as (TC − HDL-C) / HDL-C.

2.7. MRI-PDFF acquisition and region of interest (ROI) analysis

Hepatic fat content was quantified using magnetic resonance proton density fat fraction (MRI-PDFF). Scans were performed on a 3.0 T MRI scanner (Philips Ingenia 3.0T CX) equipped with a standard body coil. Participants underwent supine upper abdominal scanning following an 8-hour fast. The liver was segmented according to the Couinaud classification: segment I (caudate lobe), segment II (left lateral superior segment), segment III (left lateral inferior segment), segment IV (left medial segment), segment V (anterior inferior segment), segment VI (posterior inferior segment), segment VII (posterior superior segment), and segment VIII (anterior superior segment). Two experienced radiologists manually defined circular ROIs (100 mm^2 for segment I, 200–300 mm^2 for other segments) in a double-blind manner, avoiding imaging artifacts, organ boundaries, major intrahepatic vessels, and bile ducts. For each segment, three ROIs were placed in areas with the highest estimated fat content, avoiding vessels, bile ducts, and artifact regions. Measurements from the three ROIs per segment were averaged.

2.8. Fecal microbiome analysis and functional prediction

Total genomic DNA was extracted from fecal samples using the FastDNA Spin Kit for Feces (MP Biomedicals, Irvine, CA, USA) according to the manufacturer's instructions. The hypervariable V3-V4 region of the bacterial 16S rRNA gene was amplified via polymerase chain reaction (PCR) using the universal primer pair 341F/806R. The resulting amplicons were visualized and separated by electrophoresis on a 1.5% agarose gel. Target DNA bands were excised and purified using the DNA Gel/PCR Purification Miniprep Kit (Invitrogen Ambion, USA). Sequencing was performed on the Illumina MiSeq PE300 platform (Illumina, San Diego, CA, USA). Subsequent bioinformatic processing, including quality filtering, read pairing, and taxonomic assignment, was conducted using the QIIME 2 pipeline. Within-sample microbial diversity (α-diversity) was assessed using Shannon, Chao1, Simpson, and Observed Species indices. To identify taxa with differential abundance between groups, linear discriminant analysis effect size (LEfSe) was performed on the OmicStudio online platform (https://www.omicstudio.cn/tool). Phylogenetic Investigation of Communities by Reconstruction of Unobserved States (PICRUSt2) was used to predict the functional profiles of gut microbial communities.

2.9. Non-targeted metabolomics analysis

Non-targeted metabolomic analyses of fecal and serum samples were conducted using liquid chromatography–tandem mass spectrometry (LC-MS/MS). Sample separation was performed using a UHPLC system (Vanquish, Thermo Scientific, Waltham, MA, USA) equipped with a U3000 RSLC series analytical column (Thermo Scientific). The separated metabolites were analyzed on a high-resolution Q-Exactive HF-X mass spectrometer (Thermo Scientific, Waltham, MA, USA) operating in both positive and negative ionization modes. Raw data files were processed for peak picking, alignment, and compound identification.

Pathway enrichment analysis of the identified significant metabolites was performed using MetaboAnalyst (https://www.metaboanalyst.ca).

2.10. Statistical analysis

Statistical analyses and graphical representations were performed using SPSS version 27.0 (SPSS Inc., Chicago, IL, USA) and GraphPad Prism 10.4.2 (GraphPad Software, USA). Quantitative data are expressed as mean ± standard error (SE). Data normality was assessed using the Shapiro-Wilk test ($P > 0.05$ as the normality criterion). Intergroup comparisons employed the independent sample t-test (for normally distributed data) or the Wilcoxon rank-sum test (for non-normally distributed data). Intragroup comparisons were performed using paired t-tests (for normally distributed data) or Wilcoxon signed-rank tests (for non-normally distributed data). Correlation analysis between variables was conducted using Spearman's correlation analysis. Gephi 0.10 software was used to visualize correlation network diagrams. $P < 0.05$ was considered statistically significant.

3. Results

3.1. Baseline characteristics of participants

The study design and participant flow are detailed in the CONSORT diagram (Figure 1). Initially, 120 individuals were recruited, four failed to meet the eligibility criteria and were excluded. During the follow-up period, eight participants from both the *B. adolescentis* CCFM1061 supplementation group and the placebo group withdrew from the study. Consequently, 50 subjects in each group completed the trial and were included in the per-protocol analysis. Baseline demographic and clinical characteristics of the enrolled participants are summarized in Table 1. Comparative analysis revealed no statistically significant differences in any measured parameters between the CCFM1061 and placebo groups at baseline.

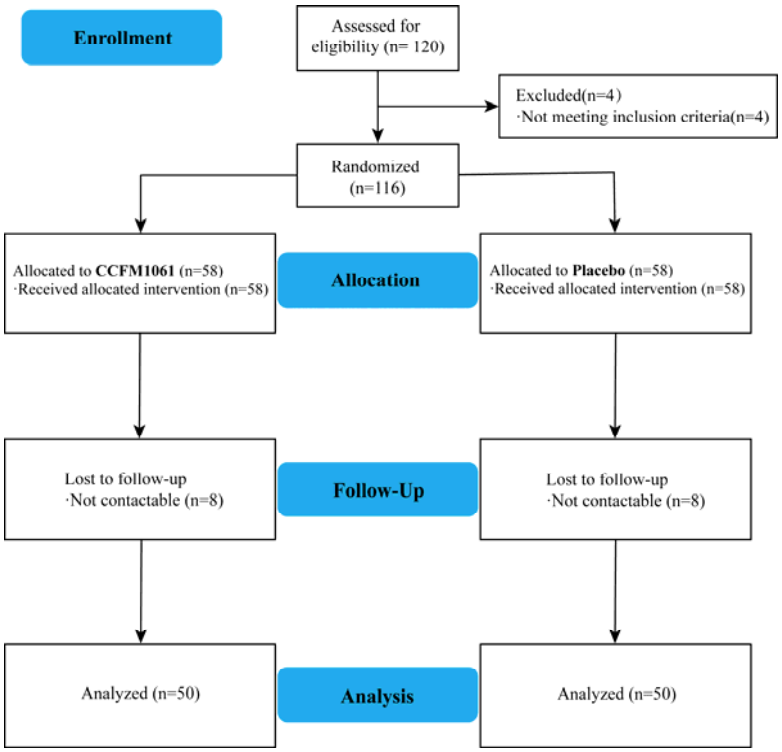


Figure 1 CONSORT study flow chart.

Table 1 Baseline characteristics of participants.

Characteristics	Placebo(N=50)	CCFM1061(N=50)	P-value
Age (years)	47.30±11.18	43.74±10.43	0.085^{NS}
Male/Female	23/27	30/20	0.136^{NS}
BMI (kg·m^{-2})	26.14±3.05	26.94±3.17	0.236^{NS}
AST (IU/L)	23.62±9.46	24.71±8.31	0.199^{NS}
ALT (IU/L)	33.59±21.92	38.96±22.34	0.222^{NS}
GGT (IU/L)	38.25±22.19	47.78±34.28	0.207^{NS}
TG (mmol/L)	2.21±1.17	2.34±1.73	0.424^{NS}
TC (mmol/L)	5.21±0.82	5.11±1.01	0.501^{NS}
HDL-C (mmol/L)	1.16±0.21	1.05±0.18	0.066^{NS}
LDL-C (mmol/L)	3.10±0.75	3.12±0.92	0.764^{NS}
FFA (mmol/L)	0.36±0.18	0.35±0.13	0.473^{NS}
AI	3.81±1.03	4.14±1.22	0.203^{NS}
GLU (mmol/L)	6.07±1.41	5.64±0.56	0.669^{NS}
hs-CRP (mg/L)	2.77±3.99	2.82±5.63	0.754^{NS}
HbA1c (%)	5.95±0.97	5.63±0.42	0.328^{NS}
In (μIU/mL)	12.69±5.72	13.33±4.05	0.092^{NS}
Segment I (%)	10.11±6.72	11.08±6.38	0.365^{NS}
Segment II (%)	10.84±6.85	12.05±6.46	0.195^{NS}
Segment III (%)	11.88±7.43	12.84±6.88	0.352^{NS}
Segment IV (%)	11.80±7.16	13.34±7.05	0.138^{NS}
Segment V (%)	11.48±7.59	13.74±7.57	0.102^{NS}
Segment VI (%)	10.74±7.47	12.93±7.68	0.114^{NS}
Segment VII (%)	10.70±7.58	13.34±8.04	0.081^{NS}
Segment VIII (%)	11.27±7.88	13.71±7.59	0.056^{NS}

NS, not significant; N, number of participants; BMI, body mass index; AST, aspartate aminotransferase; ALT, alanine aminotransferase; GGT, γ-glutamyl transferase; TG, triglyceride; TC, total Cholesterol; HDL-C, high-density lipoprotein cholesterol; LDL-C, low-density lipoprotein cholesterol; FFA, free fatty acid; AI, atherosclerosis index; GLU, glucose; hs-CRP, high-sensitivity c-reactive protein; HbA1c, glycated hemoglobin; In, insulin; Segment I, caudate lobe; Segment II, left lateral superior segment; Segment III, left lateral inferior segment; Segment IV, left medial segment; Segment V, anterior inferior segment; Segment VI, posterior inferior segment; Segment VII, posterior superior segment; Segment VIII, anterior superior segment.

3.2. CCFM1061 significantly reduced hepatic fat accumulation following intervention but exerted no apparent effect on blood parameters

The experimental procedure is illustrated in Figure 2A. Regarding changes in hepatic lipid accumulation, quantitative MRI-PDFF results demonstrated that after 13 weeks of intervention, *B. adolescentis* CCFM1061 significantly reduced hepatic lipid deposition (Figure S2). Specifically, within-group comparisons demonstrated statistically significant reductions in hepatic fat percentage from baseline to post-intervention across all eight liver segments (segments I–VIII) in the CCFM1061 group (all $P < 0.01$; Figure 2B–I). In contrast, no statistically significant within-group changes in hepatic fat content were observed in any liver segment in the placebo group (all $P > 0.05$). Further intergroup comparisons revealed that the reduction in hepatic fat in segments II, V, VI, and VII were significantly greater in the CCFM1061 group relative to the placebo group ($P < 0.05$).

No notable differences emerged between the CCFM1061 and placebo groups in the post-intervention evaluation of glucose and lipid metabolism. Specifically, the levels of hepatic function indicators (AST, ALT, GGT), circulating lipids (TG, TC, HDL-C, LDL-C, FFA, AI), and Inflammation + glycemic parameters (GLU, hs-CRP, HbA1c, insulin) remained comparable after the 13-week intervention (Figure 3A-M).

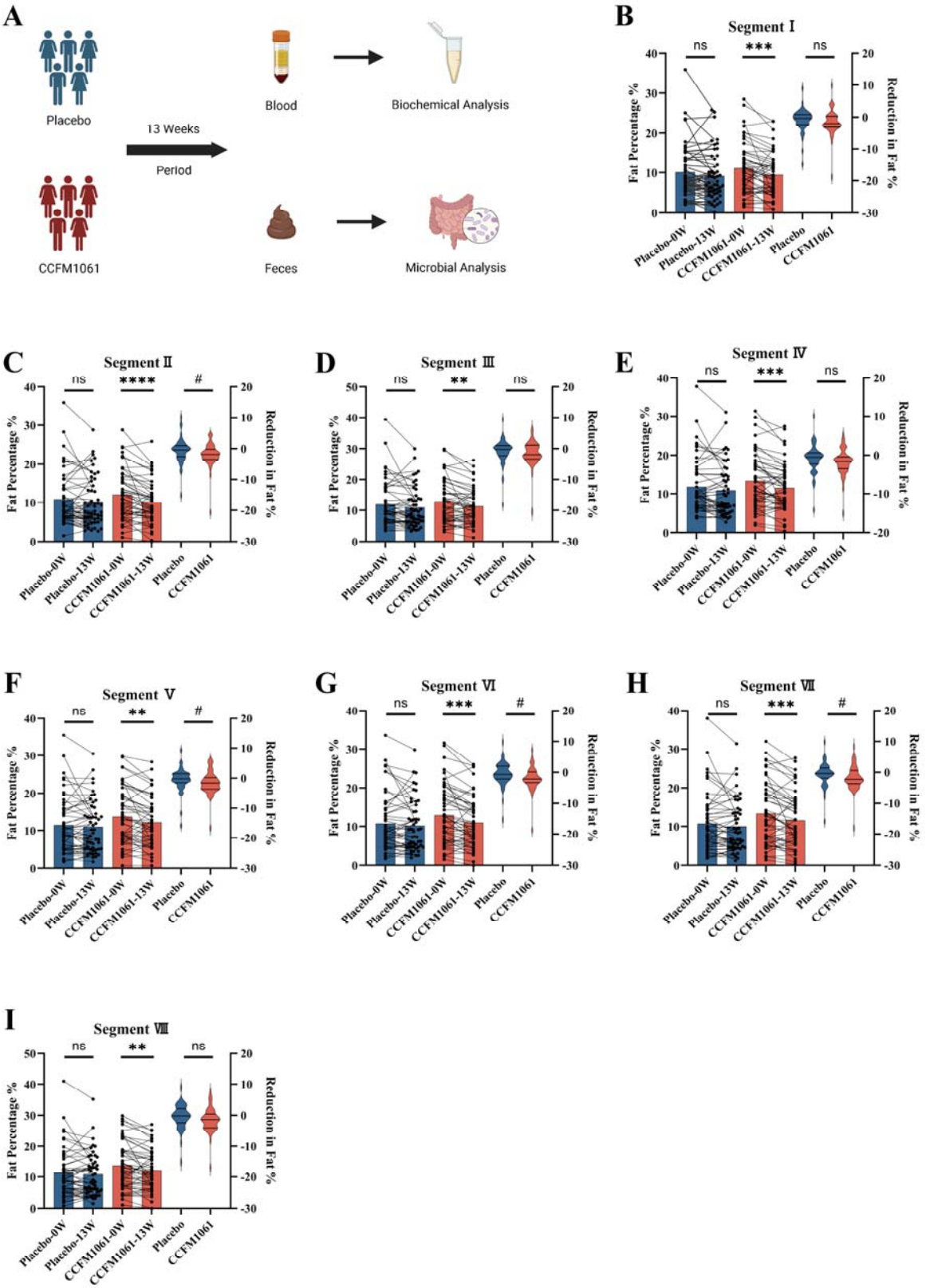


Figure 2 Sample processing flow(A) and the effect of *B. adolescentis* CCFM1061 on clinical indicators of hepatic segments. (B) Caudate lobe. (C) Left lateral superior segment. (D) Left lateral inferior segment. (E) Left medial segment. (F) Anterior inferior segment. (G) Posterior inferior segment. (H) Posterior superior segment. (I) Anterior superior segment. **P* < 0.05; ***P* < 0.01; ****P* < 0.001; *****P* < 0.0001 indicate significant differences compared with baseline within the same group; #*P* < 0.05 indicate significant differences in the reduction of hepatic fat accumulation between the CCFM1061 and the placebo group pre- and post-intervention; ns, not significant.

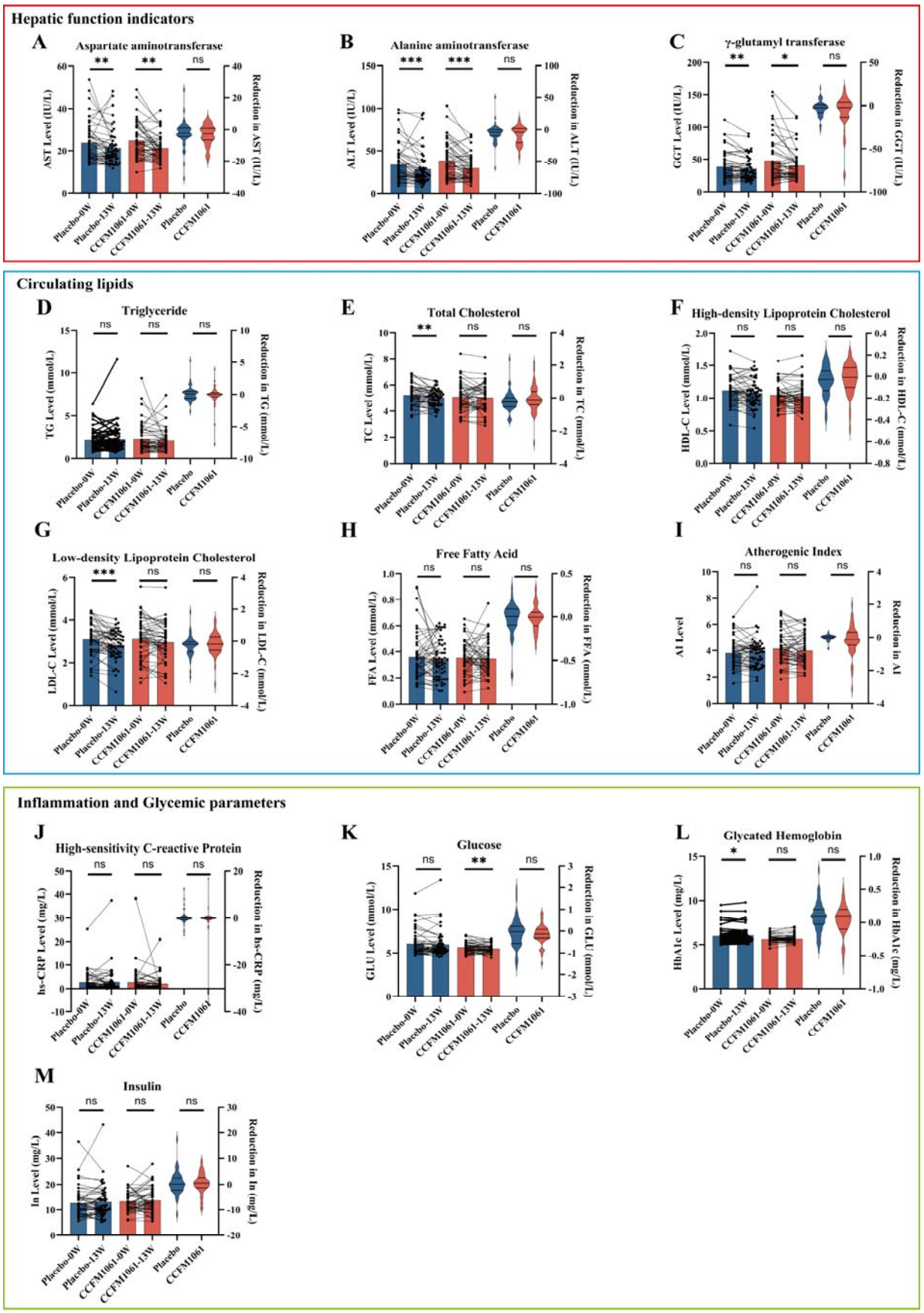


Figure 3 The effect of *B. adolescentis* CCFM1061 on glucolipid metabolism in participants. (A) Aspartate aminotransferase. (B) Alanine aminotransferase. (C) γ-glutamyl transferase. (D) Triglyceride. (E) Total cholesterol. (F) High-density lipoprotein cholesterol. (G) Low-density lipoprotein cholesterol. (H) Free fatty acid. (I) Atherogenic index. (J) Glucose. (K) High-sensitivity C-reactive protein. (L) Glycated hemoglobin. (M) Insulin. *P < 0.05; **P < 0.01; ***P < 0.001 indicate significant differences compared with baseline within the same group; ns, not significant.

3.3. CCFM1061 modulates gut microbiota structure and promotes functional amelioration of beneficial bacteria post-intervention.

To determine whether CCFM1061 supplementation altered the structure of the gut microbial community, fecal samples obtained from participants following the intervention period were subjected to 16S rRNA gene sequencing.

With respect to community structure, principal coordinate analysis (PCoA) using Bray–Curtis distance (Figure 4A) demonstrated a significant divergence in gut microbiota composition between the CCFM1061 and placebo groups (P = 0.035), despite considerable intra-group variability (R = 0.0257). Consistent with this finding, PCA analysis also revealed significant differences between the two groups (P = 0.005) (Figure 4B). However, α-diversity indices (including Shannon, Chao1, Simpson, and Observed Species) showed no significant differences between groups (Figure 4C-F), indicating that CCFM1061 did not significantly alter overall microbial abundance or evenness, but rather specifically modulated the composition of particular microbial communities.

To characterize this compositional shift, analysis at the phylum taxonomic rank (Figure 4G) revealed that the CCFM1061 group displayed a significantly elevated relative abundance of Bacteroidetes relative to the placebo group. Conversely, the abundances of Firmicutes and Actinobacteria were concurrently reduced. To further identify the specific microbial groups driven by CCFM1061 intervention, we performed LEfSe analysis based on the criteria LDA > 3 and $P < 0.05$ (Figure 4H–I). Relative to the placebo, supplementation with CCFM1061 induced significant alterations in gut microbiota composition at the genus level. The intervention group demonstrated marked enrichment of several beneficial genera, most prominently *Bacteroides* (LDA = 4.59). Other enriched genera included *Alistipes*, *Paraprevotella*, *Megamonas*, *Dialister*, and the *Eubacterium coprostanoligenes group*. Additionally, taxa known for short-chain fatty acid production, such as *Lachnospiraceae_UCG_004*, *Ruminococcus 1*, and *Ruminococcus 2*, were present at higher abundances. In contrast, the placebo group primarily enriched *Blautia*, *Tyzzerella 4*, *Veillonella*, *Desulfovibrio*, and the *Eubacterium ruminantium group*. To assess the functional implications of the altered microbial community, we predicted KEGG pathways using PICRUSt2 (Figure 4J). The analysis revealed that the CCFM1061 group exhibited 80 significantly upregulated and 22 downregulated pathways compared to the placebo ($P < 0.05$). Among the top 30 pathways, CCFM1061 supplementation was associated with enrichment of predicted microbial functional pathways involved in energy metabolism, including the citrate cycle (TCA cycle), thermogenesis, and glyoxylate and dicarboxylate metabolism. The intervention was also associated with predicted enrichment of microbial functional pathways related to metabolic regulation relevant to MAFLD, including pathways associated with PPAR signaling, degradation pathways for leucine and isoleucine, metabolic pathways for glycine, serine, and threonine, and butanoate metabolism related to short-chain fatty acid metabolism.

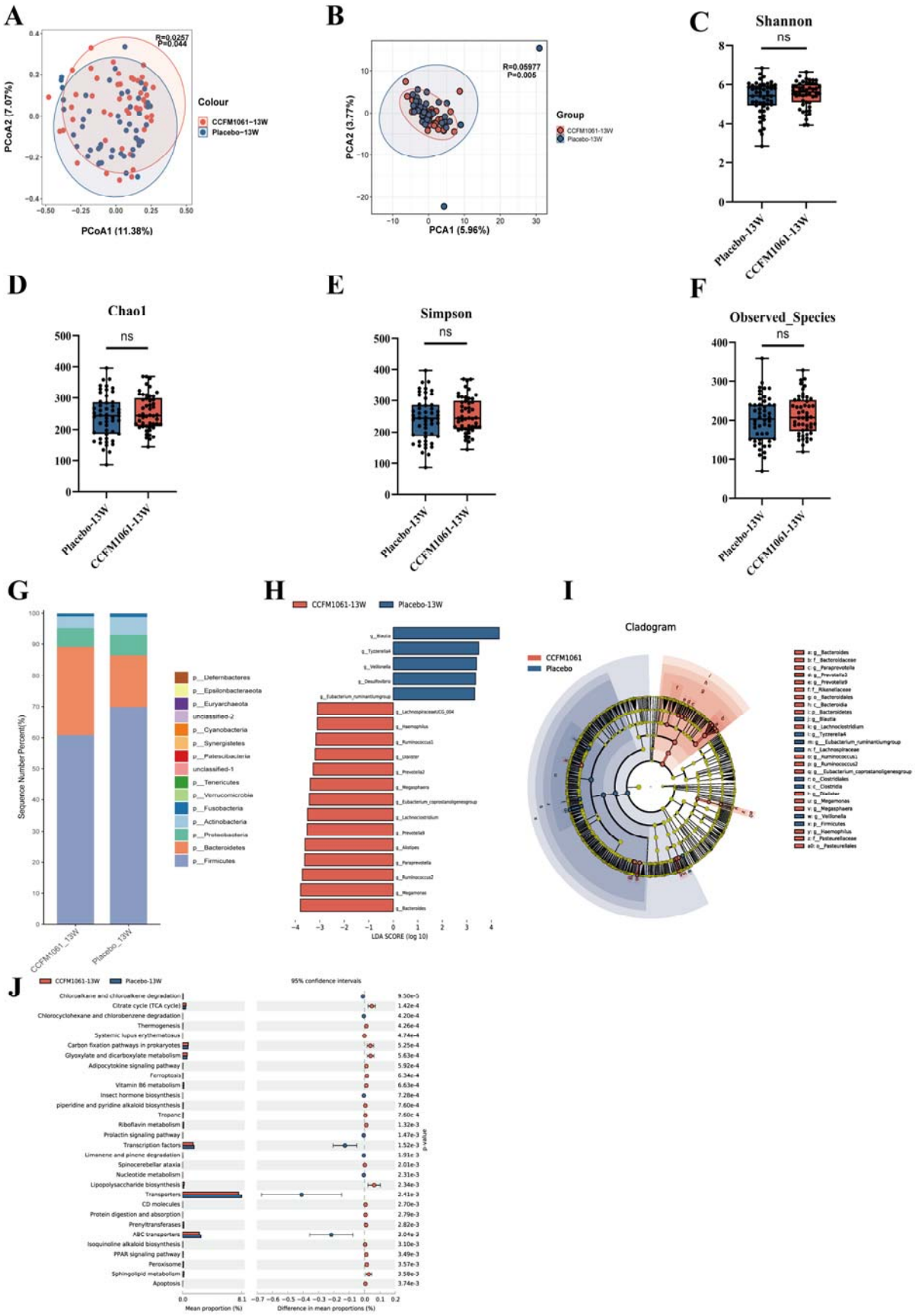


Figure 4 The effect of *B. adolescentis* CCFM1061 on the gut microbiota of participants. (A) Beta diversity. (B) PCA analysis. (C) Shannon index. (D) Chao1 richness estimator. (E) Simpson's diversity index. (F) Observed species. (G) Distribution of microbial communities at the phylum level. (H) LDA results of the gut microbiota. (I) Linear discriminant analysis effect size. (J) PICRUSt2-predicted functional metabolic pathways; All statistical comparisons shown in the figures were performed as between-group comparisons between the CCFM1061 and placebo groups at week 13 (post-intervention), and statistical significance was determined accordingly.

3.4. Multilevel regulatory effects of CCFM1061 on bile acid, amino acid, and fatty acid metabolism following intervention

To evaluate the global metabolic impact of CCFM1061, non-targeted metabolomics was performed on post-intervention serum and fecal samples. OPLS-DA models revealed clear separation from the placebo in both serum and fecal metabolomes (Figure 5A-D). These results demonstrate that the 13-week intervention was sufficient to remodel the host systemic metabolic profile.

Analysis of fecal samples revealed multiple metabolites exhibiting significant alterations in the CCFM1061 group relative to the placebo group ($Log_2FC > 1.5$, $P < 0.05$). Among these, alterations associated with bile acid metabolism were the most prominent (Figure 5E). Compared to the placebo group, fecal levels of primary bile acids—specifically taurocholic acid and taurochenodeoxycholic acid—were significantly elevated in the CCFM1061 group. Additionally, levels of multiple lipid and fatty acid derivatives were altered. Notably, unsaturated fatty acid esters with anti-inflammatory properties, such as docosahexaenoic acid ethyl ester (DHA derivative) and trans-10-heptadecenoic acid, showed significant increases. Concurrent with these changes, several amino acids and their derivatives were also elevated, including L-arginine, L-tryptophan, and leucylproline. KEGG pathway enrichment analysis of differentially metabolized compounds further corroborated these findings, with primary bile acid biosynthesis emerging as the most significantly enriched pathway. Other pathways demonstrating significant enrichment included taurine and hypotaurine metabolism, arginine biosynthesis, and arginine and proline metabolism (Figure 5F).

Serum metabolomics analysis revealed the systemic effects of CCFM1061 intervention (Figure 5G). Regarding lipid metabolism, levels of multiple saturated fatty acids in serum from the CCFM1061 group were significantly downregulated, including lauric acid, myristic acid, and pentadecanoic acid. Levels of linoleic acid, an essential fatty acid, were also markedly reduced. Importantly, a suite of dicarboxylic acids serving as markers of fatty acid ω-oxidation—notably suberic acid and azelaic acid, along with dodecanedioic acid and pimelic acid—were consistently and significantly downregulated. Regarding inflammation and oxidative stress, levels of 3-hydroxyanthranilic acid were significantly reduced, whereas adenosine and picolinic acid were significantly increased. In amino acid metabolism, the branched-chain amino acid metabolites N-acetylvaline and N-isovalerylglycine were significantly downregulated. Enrichment analysis based on KEGG pathways indicated that the intervention significantly impacted several key metabolic routes, primarily involving fatty acid biosynthesis, linoleic acid metabolism, biosynthesis of unsaturated fatty acids, purine metabolism, and tryptophan metabolism (Figure 5H).

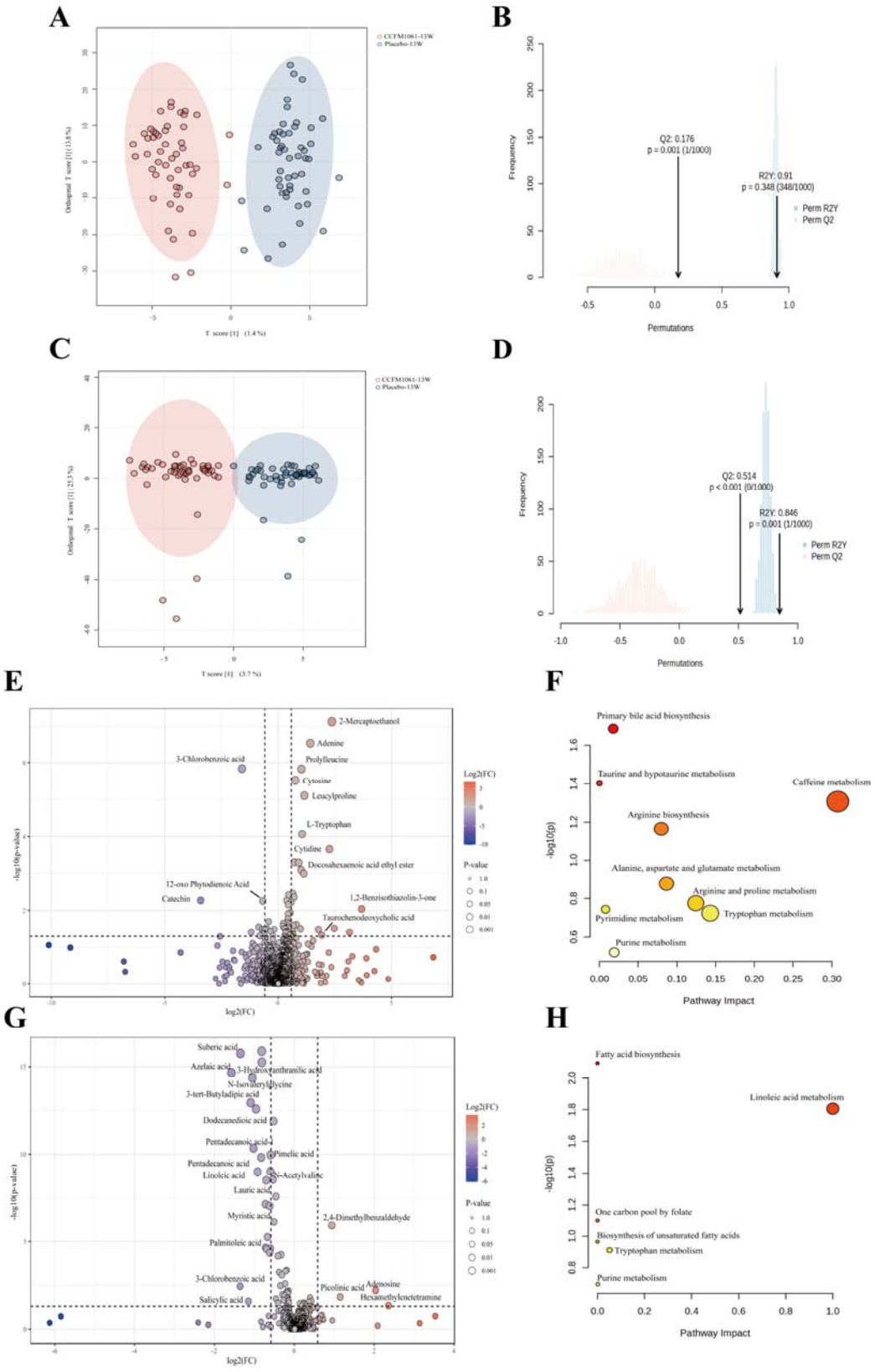


Figure 5 Orthogonal partial least squares-discriminant analysis (OPLS-DA) of non-targeted metabolomics from fecal and serum samples. (A) OPLS-DA score plot of fecal metabolites distinguishing the placebo group from the CCFM1061 group. (B) Permutation test plot (1000 iterations) of the corresponding fecal OPLS-DA model, validating the model's robustness against overfitting. (C) OPLS-DA score plot of serum metabolites. (D) Permutation test plot (1000 iterations) of the corresponding serum OPLS-DA model. (E) Significantly differentiated metabolites in non-targeted metabolomics analysis of fecal samples from CCFM1061. (F) Pathway enrichment of fecal samples from CCFM1061. (G) Significantly differentiated metabolites in non-targeted metabolomics analysis of serum samples from CCFM1061. (H) Pathway enrichment of serum samples from CCFM1061; All statistical comparisons shown in the figures represent between-group differences between the CCFM1061 and placebo groups at week 13 (post-intervention).

3.5. CCFM1061 Multi-Omics Correlation Analysis Results

Using the Spearman correlation network diagram ($|r| > 0.3$, $P < 0.05$), To further explore host–microbe metabolic interactions, a multi-omics correlation analysis was performed integrating LEfSe-identified gut microbial genera with differential untargeted metabolites from both fecal and serum samples, as well as hepatic fat content in liver segments II, V, VI, and VII, which showed significant reductions in lipid accumulation compared with the placebo group in Section 3.2, thereby revealing potential functional links among microbial taxa, serum/fecal metabolites, and region-specific hepatic lipid deposition (Figure 6). The results showed that several beneficial genera enriched in the CCFM1061 group were positively correlated with a series of beneficial metabolites. Among these, the genera *Eubacterium*, *Lachnospiraceae_UCG_004*, *Haemophilus*, and *Lachnoclostridium* were positively correlated with the anti-inflammatory lipid docosahexaenoic acid ethyl ester (a DHA derivative). In addition, *Ruminococcus_2* was positively correlated with trans-10-heptadecenoic acid, while *Paraprevotella* and *Lachnoclostridium* showed positive correlations with the plant-derived compounds catechin and hesperetin. Correlation analysis between fecal and serum metabolites revealed key metabolic pathways linking the gut to systemic circulation. Notably, fecal taurochenodeoxycholic acid exhibited significant negative correlations with multiple serum fatty acid ω-oxidation markers, including azelaic acid, suberic acid, and dodecanedioic acid. Taurocholic acid was also negatively correlated with serum pimelic acid and pentadecanoic acid. Furthermore, serum N-acetylvaline, a metabolite of branched-chain amino acids exhibited a positive correlation with fecal L-arginine as well as several microbiota-associated peptide metabolites.

To directly assess the relationship between metabolic changes and clinical outcomes, we correlated differentially expressed metabolites with liver fat percentage measured by MRI-PDFF. Serum metabolite–liver phenotype analysis indicated that lauric acid and N-acetylvaline were significantly negatively correlated with hepatic fat content in segment VI and segment VII, respectively. Meanwhile, fecal metabolite–liver phenotype analysis showed that cytosine and N-acetylaspartic acid were significantly positively correlated with hepatic fat content in segment VII.

In summary, multi-omics correlation analysis constructed a network linking gut microbiota to fecal metabolites, then to serum metabolites, and ultimately to hepatic fat deposition—the core clinical phenotype. This network suggests that beneficial bacteria enriched by CCFM1061 intervention are positively associated with favorable metabolic changes. The multi-omics correlation analysis revealed an inverse relationship between the modulation of intestinal bile acid metabolism and the enhancement of systemic fatty acid oxidation. Ultimately, improvements in key circulating lipid and amino acid metabolites are directly associated with reduced hepatic fat content.

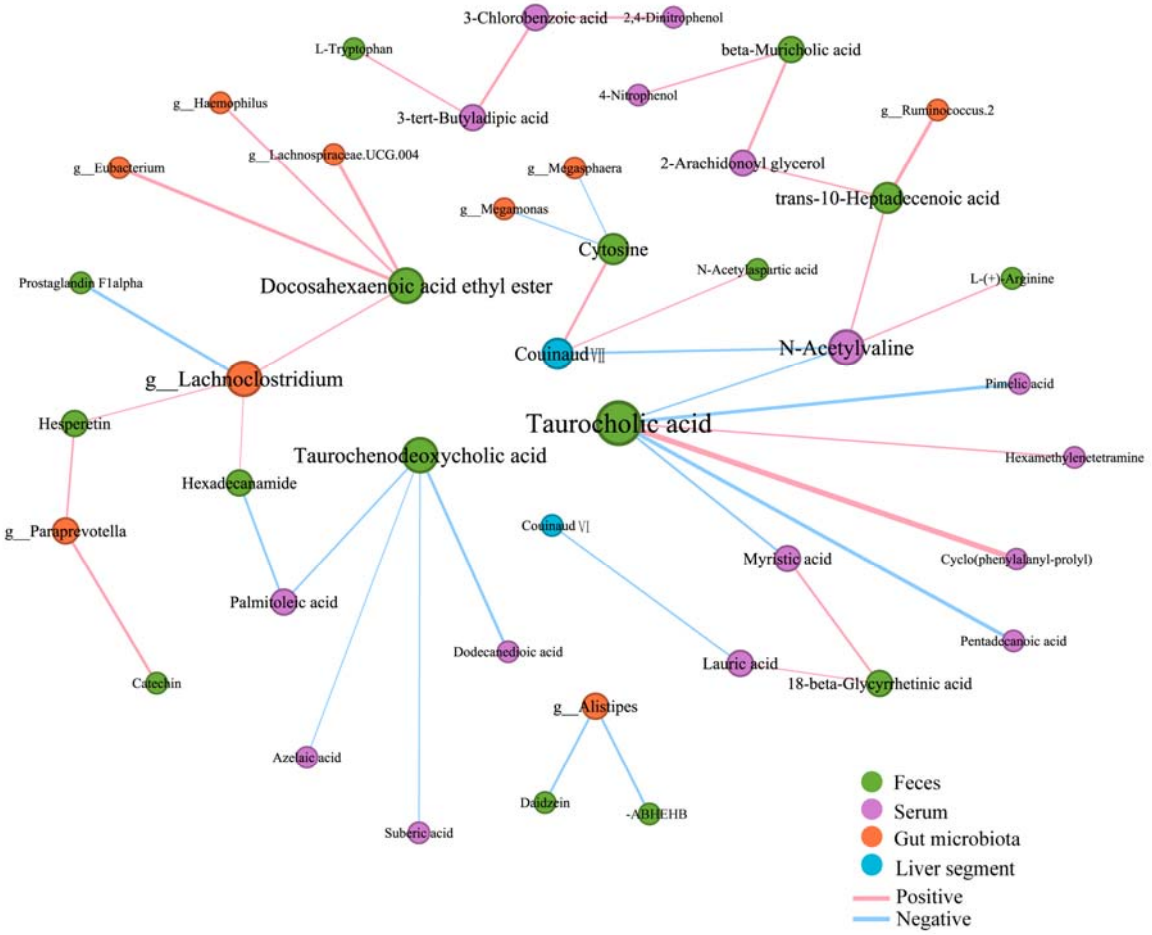


Figure 6 Spearman correlation network diagram of *B. adolescentis* CCFM1061

4. Discussion

Given that hepatic fat content is one of the key reference standards for the diagnosis and staging of metabolic dysfunction-associated fatty liver disease (MAFLD), and considering the marked spatial heterogeneity of hepatic fat deposition—as well as the variability in response rate and magnitude among different liver segments to therapeutic interventions[29,30]—the present study employed magnetic resonance imaging–proton density fat fraction (MRI-PDFF) to perform a microanatomical assessment of hepatic lipid distribution in patients with MAFLD. The results demonstrated that intervention with *Bifidobacterium adolescentis* CCFM1061 led to observable reductions in fat accumulation across multiple hepatic segments. Furthermore, multidimensional integration of gut microbiota and metabolomics data suggested that CCFM1061 may primarily influence hepatic lipid deposition by modulating gut microbial composition and gut-derived metabolic signals, thereby contributing to localized improvements in hepatic lipid handling.

The microbiome-level findings provide an ecological basis for the aforementioned interpretation. CCFM1061 did not induce broad alterations in overall microbial diversity; rather, it selectively enriched several genera associated with metabolic homeostasis and lipid regulation along the gut–liver axis. Among these, the genus *Alistipes*, which exhibits higher abundance in healthy individuals than in patients with MAFLD, has been reported to exert anti-inflammatory effects through modulation of the gut

microenvironment and host immune responses, and to alleviate metabolic disturbances in experimental models of fatty liver[31]. *Megamonas* has likewise been considered a microbiota target with regulatory potential in MAFLD, with existing evidence indicating its involvement in lipid and energy metabolism dysregulation along the gut–liver axis [32]. In addition, the *Eubacterium coprostanoligenes group* is negatively correlated with serum and fecal cholesterol levels and may reduce host lipid burden by converting cholesterol into the non-absorbable metabolite coprostanol[33]. The enrichment of the key short-chain fatty acid–producing taxon *Lachnospiraceae_UCG-004* further supports an enhanced capacity for gut-derived metabolite production, particularly butyrate, reflecting a functional remodeling of the gut microbiota associated with improvements in host metabolic status[34].

Notably, the abundance of *Bacteroides*, a genus characterized by strong polysaccharide-degrading capacity, was significantly increased following CCFM1061 intervention. Previous studies have demonstrated that *Bacteroides* species can attenuate inflammatory signaling, enhance short-chain fatty acid production, and suppress the expression of host genes involved in hepatic lipogenesis in animal models[35,36]. In addition, certain *Bacteroides* strains harbor bile salt hydrolases (BSHs) with substrate-selective deconjugation activity. For instance, *Bacteroides thetaiotaomicron* has been shown to deconjugate taurine-β-muricholic acid (TβMCA), while exhibiting limited activity toward taurocholic acid (TCA)[37,38]. Taken together, these alterations in microbial abundance suggest that CCFM1061 induced a function-oriented remodeling of the gut microbiota, thereby providing an upstream ecological context for subsequent changes in gut-derived metabolic signals.

At the metabolic level, bile acids may represent a critical link connecting microbial alterations with improvements in hepatic metabolism. Following intervention, fecal taurine-conjugated bile acids, including taurocholic acid (TCA) and taurochenodeoxycholic acid (TCDCA), were significantly increased. In conjunction with the enrichment of *Bacteroides*, this finding suggests that CCFM1061 may influence microbial bile acid transformation capacity, potentially delaying the conversion of primary bile acids into secondary bile acids within the intestinal ecosystem. Beyond their classical digestive role, primary bile acids are widely recognized as signaling molecules involved in host metabolic regulation[39]. Spearman correlation network analysis further demonstrated strong negative correlations between fecal TCA and TCDCA levels and multiple dicarboxylic acids, including suberic acid and azelaic acid, which are byproducts of fatty acid ω-oxidation. Previous studies have reported that the accumulation of such dicarboxylic acids in patients with MAFLD reflects a compensatory response to impaired mitochondrial β-oxidation[40]. Moreover, these bile acids exhibited concordant associations with hepatic segments VI and VII—identified by MRI-PDFF analysis as the regions showing the most pronounced reductions in fat content—indicating consistency between metabolic homeostasis restoration and imaging-based phenotypic improvement.

In addition, coordinated microbe–metabolite interactions were observed in relation to inflammatory regulation and amino acid metabolic remodeling. Among the genera enriched following CCFM1061 intervention, *Ruminococcus_2* and *Lachnospiraceae_UCG_004* were positively correlated with anti-

inflammatory lipid mediators derived from docosahexaenoic acid (DHA). Circulating branched-chain amino acid–related metabolites, such as N-acetylvaline and N-isovalerylglycine, were decreased and negatively correlated with gut microbial pathways involved in branched-chain amino acid degradation. This pattern is consistent with previous findings that gut microbiota–mediated modulation of branched-chain amino acid metabolism contributes to improvements in insulin sensitivity and metabolic homeostasis[41], suggesting an overall amelioration of metabolic status. Taken together, the multi-omics association patterns observed in this study support a model in which CCFM1061-induced remodeling of the gut microbiota is linked to downstream metabolic adaptation along the gut–liver axis, thereby providing a coherent biological explanation for the observed reduction in hepatic lipid accumulation (Figure 7). It should be emphasized, however, that although bile acid–related signaling pathways, such as the FXR–PPAR axis, are considered to participate in the regulation of hepatic lipid oxidation and thermogenesis[42–46], these signaling cascades were not directly assessed in the present study. Accordingly, the proposed mechanisms are derived from literature evidence and multi-omics correlations and should be regarded as a conceptual framework rather than causal validation. Furthermore, the multi-omics analyses conducted herein remain inherently associative; despite the high internal consistency across data layers, targeted functional experiments, isotope tracing approaches, or interventional designs are required to elucidate the precise mechanisms linking probiotic-induced microbial remodeling with hepatic lipid metabolism.

It is noteworthy that the imaging-based improvements observed in this study were not accompanied by significant changes in conventional serum biochemical parameters, including liver function indices, lipid profiles, inflammatory markers, or glycemic indicators. This apparent “imaging–biochemistry dissociation” is increasingly recognized in MAFLD research and does not diminish the clinical relevance of the intervention. Clinical evidence indicates that in patients with mild-to-moderate MAFLD, serum transaminases and lipid parameters often remain within normal or near-normal ranges, rendering them insufficiently sensitive to detect early or localized improvements in hepatic steatosis identified through advanced imaging or histological assessment[47,48]. A similar pattern has been reported in studies involving dietary, lifestyle, and probiotic interventions, where improvements in hepatic steatosis or metabolic phenotypes precede detectable alterations in serum lipid profiles or transaminase levels[49,50]. Indeed, the limited sensitivity of circulating biomarkers in capturing early metabolic benefits has been acknowledged, and imaging- or tissue-based endpoints are increasingly regarded as more sensitive indicators for detecting early-stage or organ-specific changes in hepatic steatosis, particularly during the initial phases of disease progression[51,52]. Importantly, the alterations observed in bile acid profiles and lipid-related metabolites in the present study further support the notion that probiotic-mediated modulation of the gut–liver axis may preferentially target hepatic lipid storage and metabolic flexibility, with effects emerging prior to measurable changes in conventional blood biomarkers. Nevertheless, it should be emphasized that although the intervention duration was sufficient to detect significant reductions in hepatic fat content by MRI-PDFF, it may not have reached the temporal threshold required to induce detectable systemic biochemical changes or to fully capture downstream metabolic

adaptations. Extending the intervention period and incorporating follow-up assessments in future studies may help clarify the temporal sequence between organ-specific and systemic metabolic responses following probiotic supplementation.

Placing the present findings within the context of previous clinical studies on MAFLD further facilitates interpretation of the clinical relevance of CCFM1061. Randomized controlled trials employing MRI-PDFF as a primary endpoint have demonstrated that relatively short-term probiotic or synbiotic interventions (approximately 3 months) are sufficient to detect reductions in hepatic fat content, while conventional liver biochemical indices and other circulating parameters often remain unchanged between groups, exhibiting a pattern similar to the "imaging-sensitive yet biochemically delayed" response observed in this study[47,53]. In contrast, clinical trials with longer intervention durations, relying predominantly on indirect indices of steatosis or ultrasound-based assessments, and reporting improvements primarily in biochemical markers or composite scores, are more likely to observe reductions in transaminases or inflammatory indicators. This discrepancy suggests that the selection of outcome measures and the stage of disease may substantially influence the manifestation of clinical signals[54]. Although direct comparison of efficacy across studies is constrained by heterogeneity in strain composition, dosage, intervention duration, and baseline disease severity, the present study captured regional alterations in hepatic fat using MRI-PDFF, thereby providing higher-resolution, organ-level evidence for probiotic intervention in MAFLD. These findings further support the value of imaging-based endpoints in early-stage interventional research.

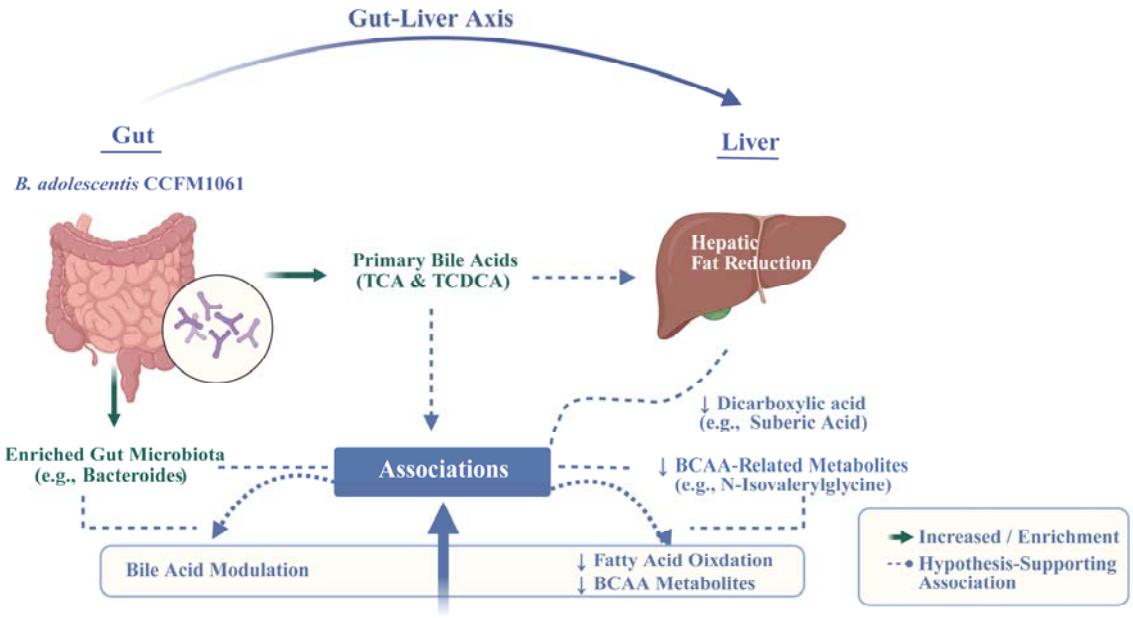


Figure 7 Speculative mechanism diagram of *B. adolescentis* CCFM1061.

5. Conclusion

This randomized, double-blind, placebo-controlled trial provides robust imaging-based evidence through multi-segment quantitative assessment using MRI-PDFF, demonstrating that supplementation with *Bifidobacterium adolescentis* CCFM1061 significantly reduces hepatic fat accumulation in patients with MAFLD. Integrated multi-omics analyses support an interpretative framework centered on the gut–liver axis:

CCFM1061 supplementation was associated with remodeling of gut microbial structure and alterations in gut-derived metabolites, particularly bile acid–related metabolites, which were linked to coordinated changes in lipid- and amino acid–related metabolic pathways. Collectively, these findings advance current understanding of probiotic–host interactions and highlight the clinical potential of CCFM1061 as a microbiota-targeted strategy for alleviating hepatic steatosis in MAFLD.

Conflicts of interest

The authors declare that they have no conflicts of interest.

Acknowledgements

This research was financially supported by the National Key R&D Program of China (2023YFC2506000/2023YFC2506004), the National Natural Science Foundation of China (No. 32272332), the Fundamental Research Funds for the Central Universities (JUSRP622020, JUSRP51501) and the Program of Collaborative Innovation Centre of Food Safety and Quality Control in Jiangsu Province.

References

[1] M. Eslam, A.J. Sanyal, J. George, A. Sanyal, B. Neuschwander-Tetri, C. Tiribelli, D.E. Kleiner, E. Brunt, E. Bugianesi, H. Yki-Järvinen, H. Grønbæk, H. Cortez-Pinto, J. George, J. Fan, L. Valenti, M. Abdelmalek, M. Romero-Gomez, M. Rinella, M. Arrese, M. Eslam, P. Bedossa, P.N. Newsome, Q.M. Anstee, R. Jalan, R. Bataller, R. Loomba, S. Sookoian, S.K. Sarin, S. Harrison, T. Kawaguchi, V.W.-S. Wong, V. Ratziu, Y. Yilmaz, Z. Younossi, MAFLD: A consensus-driven proposed nomenclature for metabolic associated fatty liver disease, Gastroenterology 158 (2020) 1999-2014.e1. https://doi.org/10.1053/j.gastro.2019.11.312.

[2] M. Eslam, P.N. Newsome, S.K. Sarin, Q.M. Anstee, G. Targher, M. Romero-Gomez, S. Zelber-Sagi, V. Wai-Sun Wong, J.-F. Dufour, J.M. Schattenberg, T. Kawaguchi, M. Arrese, L. Valenti, G. Shiha, C. Tiribelli, H. Yki-Järvinen, J.-G. Fan, H. Grønbæk, Y. Yilmaz, H. Cortez-Pinto, C.P. Oliveira, P. Bedossa, L.A. Adams, M.-H. Zheng, Y. Fouad, W.-K. Chan, N. Mendez-Sanchez, S.H. Ahn, L. Castera, E. Bugianesi, V. Ratziu, J. George, A new definition for metabolic dysfunction-associated fatty liver disease: An international expert consensus statement, J. Hepatol. 73 (2020) 202–209. https://doi.org/10.1016/j.jhep.2020.03.039.

[3] E.E. Powell, V.W.-S. Wong, M. Rinella, Non-alcoholic fatty liver disease, The Lancet 397 (2021) 2212–2224. https://doi.org/10.1016/S0140-6736(20)32511-3.

[4] J. Wang, J. Du, M. Wang, M. Jin, Z. Tang, Y. Mao, Global, regional, and national burden of NAFLD in youths and young adults aged 15–39 years, 1990–2021, its attributable risk factors, and projections to 2035: A systematic analysis of the global burden of disease study 2021, Front. Nutr. 12 (2025) 1509232. https://doi.org/10.3389/fnut.2025.1509232.

[5] N. Chalasani, Z. Younossi, J.E. Lavine, M. Charlton, K. Cusi, M. Rinella, S.A. Harrison, E.M. Brunt, A.J. Sanyal, The diagnosis and management of nonalcoholic fatty liver disease: Practice guidance from the American association for the study of liver diseases, Hepatology 67 (2018) 328–357. https://doi.org/10.1002/hep.29367.

[6] M.A. Stanislawski, C.A. Lozupone, B.D. Wagner, M. Eggesbø, M.K. Sontag, N.M. Nusbacher, M. Martinez, D. Dabelea, Gut microbiota in adolescents and the association with fatty liver: The EPOCH study, Pediatr. Res. 84 (2018) 219–227. https://doi.org/10.1038/pr.2018.32.

[7] F. Li, J. Ye, C. Shao, B. Zhong, Compositional alterations of gut microbiota in nonalcoholic fatty liver disease patients: A systematic review and meta-analysis, Lipids Health Dis. 20 (2021) 22. https://doi.org/10.1186/s12944-021-01440-w.

[8] C. Long, X. Zhou, F. Xia, B. Zhou, Intestinal barrier dysfunction and gut microbiota in non-alcoholic fatty liver disease: Assessment, mechanisms, and therapeutic considerations, Biology 13 (2024) 243. https://doi.org/10.3390/biology13040243.

[9] Y.-P. Zhuang, Y.-T. Zhang, R.-X. Zhang, H.-J. Zhong, X.-X. He, The gut-liver axis in nonalcoholic fatty liver disease: Association of intestinal permeability with disease severity and treatment outcomes, Int. J. Clin. Pract. 2022 (2022) 4797453. https://doi.org/10.1155/2022/4797453.

[10] J. Soppert, E.F. Brandt, N.M. Heussen, E. Barzakova, L.M. Blank, L. Kuepfer, M.W. Hornef, J. Trebicka, J. Jankowski, M.-L. Berres, H. Noels, Blood endotoxin levels as biomarker of nonalcoholic fatty liver disease: A systematic review and meta-analysis, Clin. Gastroenterol. Hepatol. 21 (2023) 2746–2758. https://doi.org/10.1016/j.cgh.2022.11.030.

[11] B. Zhang, F. Kuipers, J.F. De Boer, J.A. Kuivenhoven, Modulation of bile acid metabolism to improve plasma lipid and lipoprotein profiles, JCM 11 (2021) 4. https://doi.org/10.3390/jcm11010004.

[12] S. Zhang, J. Zhao, F. Xie, H. He, L.J. Johnston, X. Dai, C. Wu, X. Ma, Dietary fiber-derived short-chain fatty acids: A potential therapeutic target to alleviate obesity-related nonalcoholic fatty liver disease, Obes. Rev. 22 (2021) e13316. https://doi.org/10.1111/obr.13316.

[13] H. Zhao, J. Zhou, L. Yuan, Z. Sun, Y. Liu, X. Zhao, F. Ye, Exploring the alleviating effects of bifidobacterium metabolite lactic acid on non-alcoholic steatohepatitis through the gut-liver axis, Front. Microbiol. 15 (2025) 1518150. https://doi.org/10.3389/fmicb.2024.1518150.

[14] F. Nian, L. Wu, Q. Xia, P. Tian, C. Ding, X. Lu, *Akkermansia muciniphila* and *bifidobacterium bifidum* prevent NAFLD by regulating FXR expression and gut microbiota, J Clin Transl Hepatol 000 (2023) 000–000. https://doi.org/10.14218/JCTH.2022.00415.

[15] M. Begley, C. Hill, C.G.M. Gahan, Bile salt hydrolase activity in probiotics, Appl. Environ. Microbiol. 72 (2006) 1729–1738. https://doi.org/10.1128/AEM.72.3.1729-1738.2006.

[16] Bifidobacterium adolescentis FJSSZ23M10 modulates gut microbiota and metabolism to alleviate obesity through strain-specific genomic features - food & function (RSC publishing), (n.d.). https://pubs.rsc.org/en/content/articlelanding/2025/fo/d4fo06449f (accessed November 21, 2025).

[17] G. Wang, T. Jiao, Y. Xu, D. Li, Q. Si, J. Hao, J. Zhao, H. Zhang, W. Chen, *Bifidobacterium adolescentis* and *lactobacillus rhamnosus* alleviate non-alcoholic fatty liver disease induced by a high-fat, high-cholesterol diet through modulation of different gut microbiota-dependent pathways, Food Funct. 11 (2020) 6115–6127. https://doi.org/10.1039/C9FO02905B.

[18] G. Wang, Q. Si, S. Yang, T. Jiao, H. Zhu, P. Tian, L. Wang, X. Li, L. Gong, J. Zhao, H. Zhang, W. Chen, Lactic acid bacteria reduce diabetes symptoms in mice by alleviating gut microbiota dysbiosis and inflammation in different manners, Food Funct. 11 (2020) 5898–5914. https://doi.org/10.1039/C9FO02761K.

[19] B. Henninger, C. Kremser, S. Rauch, R. Eder, W. Judmaier, H. Zoller, H. Michaely, M. Schocke, Evaluation of liver fat in the presence of iron with MRI using T2* correction: A clinical approach, Eur. Radio. 23 (2013) 1643–1649. https://doi.org/10.1007/s00330-012-2745-2.

[20] Magnetic resonance spectroscopy of hepatic fat from fundamental to clinical applications, (n.d.). https://www.mdpi.com/2075-4418/11/5/842?utm_source=chatgpt.com (accessed October 25, 2025).

[21] Q. Gu, L. Cen, J. Lai, Z. Zhang, J. Pan, F. Zhao, C. Yu, Y. Li, C. Chen, W. Chen, Z. Shen, A meta-analysis on the diagnostic performance of magnetic resonance imaging and transient elastography in nonalcoholic fatty liver disease, Eur. J. Clin. Invest. 51 (2021) e13446. https://doi.org/10.1111/eci.13446.

[22] M. Meroni, M. Longo, P. Dongiovanni, The role of probiotics in nonalcoholic fatty liver disease: A new insight into therapeutic strategies, Nutrients 11 (2019) 2642. https://doi.org/10.3390/nu11112642.

[23] G. Paolella, Gut-liver axis and probiotics: Their role in non-alcoholic fatty liver disease, World J. Gastroenterol. 20 (2014) 15518. https://doi.org/10.3748/wjg.v20.i42.15518.

[24] Y. Ni, M. Lu, Y. Xu, Q. Wang, X. Gu, Y. Li, T. Zhuang, C. Xia, T. Zhang, X. Gou, M. Zhou, The role of gut microbiota-bile acids axis in the progression of non-alcoholic fatty liver disease, Front. Microbiol. 13 (2022) 908011. https://doi.org/10.3389/fmicb.2022.908011.

[25] M. Zhao, J. Zhao, H. Yang, Z. Ouyang, C. Lv, Z. Geng, J. Zhao, The bile acid-gut microbiota axis: A central hub for physiological regulation and a novel therapeutic target for metabolic diseases, Biomed. Pharmacother. 188 (2025) 118182. https://doi.org/10.1016/j.biopha.2025.118182.

[26] A. Tyagi, V. Kumar, The gut microbiota-bile acid axis: A crucial regulator of immune function and metabolic health, World J. Microbiol. Biotechnol. 41 (2025) 215. https://doi.org/10.1007/s11274-025-04395-7.

[27] C. Chu, J. Jiang, L. Yu, Y. Li, S. Zhang, W. Zhou, Q. Wang, J. Zhao, Q. Zhai, F. Tian, W. Chen, *Bifidobacterium longum* CCFM1077 attenuates hyperlipidemia by modulating the gut microbiota composition and fecal metabolites: A randomized, double-blind, placebo-controlled clinical trial, Engineering 28 (2023) 193–205. https://doi.org/10.1016/j.eng.2023.04.010.

[28] R. Xiao, Y. Chen, X. Zhu, L. Wang, P. Tian, X. Jin, M. Liang, Z. Chen, T. Zhang, L. Qian, Q. Wang, J. Zhao, H. Zhang, G. Wang, A randomised double-blind placebo-controlled trial of a probiotic combination for manipulating the gut microbiota and managing metabolic syndrome, Food Biosci. 59 (2024) 104076. https://doi.org/10.1016/j.fbio.2024.104076.

[29] S. Ben-Moshe, S. Itzkovitz, Spatial heterogeneity in the mammalian liver, Nat. Rev. Gastroenterol. Hepatol. 16 (2019) 395–410. https://doi.org/10.1038/s41575-019-0134-x.

[30] A.A. Santos, T.C. Delgado, V. Marques, C. Ramirez-Moncayo, C. Alonso, A. Vidal-Puig, Z. Hall, M.L. Martínez-Chantar, C.M.P. Rodrigues, Spatial metabolomics and its application in the liver, Hepatology 79 (2024) 1158–1179. https://doi.org/10.1097/HEP.0000000000000341.

[31] C. Yang, J. Xu, X. Xu, W. Xu, B. Tong, S. Wang, R. Ji, Y. Tan, Y. Zhu, Characteristics of gut microbiota in patients with metabolic associated fatty liver disease, Sci. Rep. 13 (2023) 9988. https://doi.org/10.1038/s41598-023-37163-4.

[32] F. Huang, B. Lyu, F. Xie, F. Li, Y. Xing, Z. Han, J. Lai, J. Ma, Y. Zou, H. Zeng, Z. Xu, P. Gao, Y. Luo, L. Bolund, G. Tong, X. Fengping, From gut to liver: Unveiling the differences of intestinal microbiota in NAFL and NASH patients, Front. Microbiol. 15 (2024). https://doi.org/10.3389/fmicb.2024.1366744.

[33] C. Visuthranukul, S. Sriswasdi, S. Tepaamorndech, S. Chamni, A. Leelahavanichkul, Y. Joyjinda, V. Aksornkitti, S. Chomtho, Enhancing gut microbiota and microbial function with inulin supplementation in children with obesity, Int. J. Obes. 48 (2024) 1696–1704. https://doi.org/10.1038/s41366-024-01590-8.

[34] D. Zhang, Y.-P. Jian, Y.-N. Zhang, Y. Li, L.-T. Gu, H.-H. Sun, M.-D. Liu, H.-L. Zhou, Y.-S. Wang, Z.-X. Xu, Short-chain fatty acids in diseases, Cell Commun. Signaling 21 (2023) 212. https://doi.org/10.1186/s12964-023-01219-9.

[35] C. Sun, X. Xiong, M. Liu, Q. Liang, Q. Zhao, G. Wei, J. Shi, X. Li, Bacteroides ovatus alleviates high-fat and high-cholesterol -induced nonalcoholic fatty liver disease via gut-liver axis, Biomedicine & Pharmacotherapy 178 (2024) 117156. https://doi.org/10.1016/j.biopha.2024.117156.

[36] H. Li, X.-K. Wang, M. Tang, L. Lei, J.-R. Li, H. Sun, J. Jiang, B. Dong, H.-Y. Li, J.-D. Jiang, Z.-G. Peng, Bacteroides thetaiotaomicron ameliorates mouse hepatic steatosis through regulating gut microbial composition, gut-liver folate and unsaturated fatty acids metabolism, Gut Microbes 16 (n.d.) 2304159. https://doi.org/10.1080/19490976.2024.2304159.

[37] L. Yao, S.C. Seaton, S. Ndousse-Fetter, A.A. Adhikari, N. DiBenedetto, A.I. Mina, A.S. Banks, L. Bry, A.S. Devlin, A selective gut bacterial bile salt hydrolase alters host metabolism, eLife 7 (n.d.) e37182. https://doi.org/10.7554/eLife.37182.

[38] Z. Song, Y. Cai, X. Lao, X. Wang, X. Lin, Y. Cui, P.K. Kalavagunta, J. Liao, L. Jin, J. Shang, J. Li, Taxonomic profiling and populational patterns of bacterial bile salt hydrolase (BSH) genes based on worldwide human gut microbiome, Microbiome 7 (2019) 9. https://doi.org/10.1186/s40168-019-0628-3.

[39] S.A. Joyce, D. O'Malley, Bile acids, bioactive signalling molecules in interoceptive gut-to-brain communication, J Physiol 600 (2022) 2565–2578. https://doi.org/10.1113/JP281727.

[40] R. Gambino, G. Musso, M. Cassader, Redox balance in the pathogenesis of nonalcoholic fatty liver disease: Mechanisms and therapeutic opportunities, Antioxid. Redox Signaling 15 (2011) 1325–1365. https://doi.org/10.1089/ars.2009.3058.

[41] J. Gojda, M. Cahova, Gut microbiota as the link between elevated BCAA serum levels and insulin resistance, Biomolecules 11 (2021) 1414. https://doi.org/10.3390/biom11101414.

[42] I. Pineda Torra, T. Claudel, C. Duval, V. Kosykh, J.-C. Fruchart, B. Staels, Bile acids induce the expression of the human peroxisome proliferator-activated receptor alpha gene via activation of the farnesoid X receptor, Mol Endocrinol 17 (2003) 259–272. https://doi.org/10.1210/me.2002-0120.

[43] S. Zhou, H. You, S. Qiu, D. Yu, Y. Bai, J. He, H. Cao, Q. Che, J. Guo, Z. Su, A new perspective on NAFLD: Focusing on the crosstalk between peroxisome proliferator-activated receptor alpha (PPARα) and farnesoid X receptor (FXR), Biomed Pharmacother 154 (2022) 113577. https://doi.org/10.1016/j.biopha.2022.113577.

[44] L. Goedeke, G.I. Shulman, Therapeutic potential of mitochondrial uncouplers for the treatment of metabolic associated fatty liver disease and NASH, Mol. Metab. 46 (2021) 101178. https://doi.org/10.1016/j.molmet.2021.101178.

[45] H.S. Park, J.E. Jang, M.S. Ko, S.H. Woo, B.J. Kim, H.S. Kim, H.S. Park, I.S. Park, E.H. Koh, K.U. Lee, Statins increase mitochondrial and peroxisomal fatty acid oxidation in the liver and prevent non-alcoholic steatohepatitis in mice, Diabetes Metab J 40 (2016) 376–385. https://doi.org/10.4093/dmj.2016.40.5.376.

[46] S.-W. Weng, J.-C. Wu, F.-C. Shen, Y.-H. Chang, Y.-J. Su, W.-S. Lian, M.-H. Tai, C.-H. Su, J.-H. Chuang, T.-K. Lin, C.-W. Liou, T.-H. Chu, Y.-H. Kao, F.-S. Wang, P.-W. Wang, Chaperonin counteracts diet-induced non-alcoholic fatty liver disease by aiding sirtuin 3 in the control of fatty acid oxidation, Diabetologia 66 (2023) 913–930. https://doi.org/10.1007/s00125-023-05869-9.

[47] S.B. Ahn, D.W. Jun, B.-K. Kang, J.H. Lim, S. Lim, M.-J. Chung, Randomized, double-blind, placebo-controlled study of a multispecies probiotic mixture in nonalcoholic fatty liver disease, Sci. Rep. 9 (2019) 5688. https://doi.org/10.1038/s41598-019-42059-3.

[48] C. Xie, D. Halegoua-DeMarzio, Role of probiotics in non-alcoholic fatty liver disease: Does gut microbiota matter?, Nutrients 11 (2019) 2837. https://doi.org/10.3390/nu11112837.

[49] T. Rosenzweig, N. Skalka, K. Rozenberg, U. Elyasiyan, A. Pinkus, B. Green, M. Stanevsky, E. Drori, Red wine and wine pomace reduced the development of insulin resistance and liver steatosis in HFD-fed mice, J. Funct. Foods 34 (2017) 379–389. https://doi.org/10.1016/j.jff.2017.04.043.

[50] S. Nabavi, M. Rafraf, M. Somi, A. Homayouni-Rad, M. Asghari-Jafarabadi, Probiotic yogurt improves body mass index and fasting insulin levels without affecting serum leptin and adiponectin levels in non-alcoholic fatty liver disease (NAFLD), J. Funct. Foods 18 (2015) 684–691. https://doi.org/10.1016/j.jff.2015.08.031.

[51] A.J. Sanyal, S.L. Friedman, A.J. McCullough, L. Dimick-Santos, Challenges and opportunities in drug and biomarker development for nonalcoholic steatohepatitis: Findings and recommendations from an American association for the study of liver diseases–U.S. food and drug administration joint workshop, Hepatology 61 (2015) 1392–1405. https://doi.org/10.1002/hep.27678.

[52] C. Caussy, S.B. Reeder, C.B. Sirlin, R. Loomba, Noninvasive, quantitative assessment of liver fat by MRI-PDFF as an endpoint in NASH trials, Hepatology 68 (2018) 763–772. https://doi.org/10.1002/hep.29797.

[53] S. Ferolla, C. Couto, L. Costa-Silva, G. Armiliato, C. Pereira, F. Martins, M. Ferrari, E. Vilela, H. Torres, A. Cunha, T. Ferrari, Beneficial effect of synbiotic supplementation on hepatic steatosis and anthropometric parameters, but not on gut permeability in a population with nonalcoholic steatohepatitis, Nutrients 8 (2016) 397. https://doi.org/10.3390/nu8070397.

[54] T. Eslamparast, H. Poustchi, F. Zamani, M. Sharafkhah, R. Malekzadeh, A. Hekmatdoost, Synbiotic supplementation in nonalcoholic fatty liver disease: A randomized, double-blind, placebo-controlled pilot study, The American Journal of Clinical Nutrition 99 (2014) 535–542. https://doi.org/10.3945/ajcn.113.068890.